Thermodynamic Description of 'FeO'-MgO-SiO_2 and 'FeO'-MnO-SiO_2 Melts – a Model Approach

J. Björkvall, Du Sichen and S. Seetharaman

Division of Theoretical Metallurgy, Department of Metallurgy
Royal Institute of Technology, 100 44 Stockholm, Sweden

(Received September 8, 1998; final form December 1, 1998)

ABSTRACT

Activities of the oxide components in the 'FeO'-MgO-SiO_2 and 'FeO'-MnO-SiO_2 systems have been predicted based on the information of binary systems using a thermodynamic model. The model considers the ionic melt as an oxygen-ion matrix with the cations including Si^{4+} distributed in it. The interactions between different cations in the presence of O^{2-} are considered as functions of both composition and temperature. The activities predicted by the model are in good agreement with the experimental data available in the literature.

1. INTRODUCTION

Although great efforts have been made all over the world to determine the thermodynamic properties of slags, researchers and engineers very often find that there are still too few data available for the slag systems of interest to the industry. Industrial slags are always multicomponent in nature. In most industrial practices, slag compositions vary with time. It is almost impossible to determine the thermodynamic properties for all these compositions. In order to meet the demands of process control, thermodynamic modelling for silicate melts has become even more essential.

A number of slag models are available in the literature, with varying degrees of success. The development of structure-based models has made considerable progress since the pioneering works of Toop and Samis /1/ as well as Masson /2/. These models have provided an insight into the relationship between the thermodynamic properties of silicate melts and their structures. However, the use of these models is limited, due to the lack of additional structural information, especially in the case of high silica containing melts and complex slags. On the other hand, empirical or semi-empirical models that are based on experimental information have been found to be of use in extrapolating and interpolating experimental data. Examples of this kind of model are a regular solution model /3,4/, a quasi- chemical approach /5/, an ionic "two-sublattice" model /6/ and an IRSID model /7/. Good agreement between the results of model calculation and experimental data has been reported /4-7/. Even in this kind of model, complex anionic species are used /6,7/. However, difficulties have been encountered in choosing the appropriate species /8/. The fractions of different species optimised in this way are somewhat arbitrary, as very little experimental evidence has been obtained to support them.

Some success has been achieved in predicting thermodynamic properties of multi-component solutions using solely the information of corresponding binary systems /9/. By assuming that two silicates of equal silica mole fraction mixed ideally, Richardson /9/ was able to predict the thermodynamic properties of MgO-MnO-SiO_2 melts at 1923 K in a range of silica mole fraction, 0.3 – 0.58. The calculations for the 'FeO'-MnO-SiO_2 and 'FeO'-MgO-MnO-SiO_2 systems were also successful from zero to 0.55 mole fraction of silica. However, disagreement was encountered in the case where the cationic radii were quite different. The disagreement indicates that the ideal mixing approach can only be applied to a limited number of systems. Despite the fact that Richardson's approach is simple and its applicability depends on the size difference of the cations involved, it shows the possibility of predicting thermodynamic properties of multi-component solutions based on the information of corresponding binary systems. Richardson's approach also reveals that next nearest neighbour interactions, viz., the cation interactions, play a dominant role in the solution thermodynamics.

Inspired by Richardson's approach, a research program is currently being carried out in the present laboratory to develop a thermodynamic model for the estimation of thermodynamic properties of multi-component ionic melts. A preliminary effort was made earlier /10/. In this work, a thermodynamic model to describe the activities of component oxides in complex slag systems based on a Temkin approach was put forward. The model was applied to the ternary system CaO-'FeO'-SiO_2 in order to calculate the activities of 'FeO' as a function of temperature and composition. While the model was found to be promising, the activities of 'FeO' in the ternary were still calculated based on the literature experimental data. Moreover, only the activity of one of the oxide components was considered at that time. The present study, being a continuation of the previous work /10/, aims at a refinement of the thermodynamic model for ionic melts and an examination into the reliability of the model in predicting the activities of the oxide components in ternary systems using solely the information from binary systems.

2. THERMODYNAMIC MODEL

2.1. Description of Ionic Melts

It is widely accepted that in a silicate melt all Si atoms are tetrahedrally bonded to four oxygen atoms. For solutions rich in basic oxide, the melt consists essentially of M^{2+}, O^{2+} and SiO_4^{4-} (orthosilicate) ions. As the concentration of SiO_2 increases, the SiO_4^{4-} tetrahedra start to join together, forming dimers $Si_2O_7^{6-}$, trimers $Si_3O_{10}^{8-}$, cyclic polymers and even a three-dimensional network of bridged silica tetrahedra. On the other hand, a silicate melt can also be considered as an oxygen matrix with different cations including Si^{4+} distributed in it. This approach was originally suggested by Lumsden /3/. The present model, a further development of a previous version /10/, is in line with Lumsden's formulation. The presence of basic cations such as Ca^{2+}, Fe^{2+}, Mg^{2+} and Mn^{2+}, along with Si^{4+}, will distort the oxygen matrix and determine the configuration of the ionic melt and the bond energies between different ions. The configuration of the ions and the bond energies will be functions of composition and temperature. By picturing the oxide melts in this manner, the difficulties in choosing the anionic species and the fractions of the same are avoided. While there are mutual effects between the cations and oxygen ions, the thermodynamic properties of the solution can be formulated by the consideration of the next nearest neighbour interactions, namely the interactions between the cations when oxygen ions are present.

2.2. Mathematical Formulation

A silicate melt containing m oxides, $C1_{c1}O_{a1}$, $C2_{c2}O_{a2}$,....$Ci_{ci}O_{ai}$,....$Cm_{cm}O_{am}$, is expressed as:

$$(C1^{v1}, C2^{v2}, ...Ci^{vi}, ..., Cm^{vm})_p(O^{2-})_q \tag{1}$$

where Ci^{vi} stands for cations, the superscript vi denotes the electrical charge. Even Si^{4+} ion is included in the cation group. p and q in equation (1) are stoichiometric coefficients and can be calculated by the following equations:

$$p = \sum_{i=1 \text{ to } m} X_{Ci} \cdot ci \tag{2}$$

$$q = \sum_{i=1 \text{ to } m} X_{ai} \cdot ai \tag{3}$$

Following the line of the above consideration, the thermodynamic properties of mixing can be formulated as functions of the interactions between different cations in the presence of O^{2-}. It is logical to use ionic fractions to describe the composition of a melt. The ionic fraction of cation y_i within the cation grouping is defined as:

$$y_i = \frac{N_i}{\sum_{j=1 \text{ to } m} N_j} \tag{4}$$

where N_i is the number of cation Ci^{vi} and the summation covers all the cations including Si^{4+}. The integral Gibbs energy of a solution can be expressed as:

$$G^m = \sum X_{Ci_{ci}O_{ai}} G^0_{Ci_{ci}O_{ai}} + RTp\sum(y_i \ln y_i) + G^E \tag{5}$$

where $X_{Ci_{ci}O_{ai}}$ and $G^0_{O_{ci}O_{ai}}$ represent the mole fraction and the standard Gibbs energy of oxide $Ci_{ci}O_{ai}$ respectively. As only oxygen ions occur in the anionic group, the second term corresponding to Temkin's expression /11/ for ideal entropy of mixing consists of only the contribution from the cation group. G^E in equation (5) stands for the excess Gibbs energy of mixing due to the interactions between different cations in the presence of oxygen ions. G^E is expressed as a function of both temperature and composition.

$$G^E = f(T, y_{Si^{4+}}) + \sum_{i=1 \text{ to } m-1} \left(\sum_{j=i+1 \text{ to } m} y_i y_j \Omega^{ij(O)} \right) \qquad (6)$$

$\Omega^{ij(O)}$ in equation (6) represents the interaction between cations Ci^{ν_i} and Cj^{ν_j} when O^{2-} ions are present. This interaction is a function of temperature and composition:

$$\Omega^{ij(O)} = \Omega_1^{ij(O)} + \Omega_2^{ij(O)} T + \left(\Omega_3^{ij(O)} + \Omega_4^{ij(O)} T \right)(y_i - y_j) + \left(\Omega_5^{ij(O)} + \Omega_6^{ij(O)} T \right)(y_i - y_j)^2 + \ldots \qquad (7)$$

The function $f(T, y_{Si^{4+}})$ in eq. (6) is intended to take account of the fact that when the hypothetical standard state for silica is adopted, the excess Gibbs energy is not zero as the composition approaches pure SiO_2. However, this function can only be evaluated on the basis of the experimental data for the compositions of very high silica contents. In view of the fact that the highest silica contents in all systems studied in this work are below 0.55, $f(T, y_{Si^{4+}})$ is arbitrarily set to zero. Further investigation based on well established experimental data is required before this function can be obtained.

The present approach is very similar to that suggested by Hillert *et al.* in their thermodynamic representation /6/. It is noted that only binary interaction terms are present in the excess Gibbs energy of mixing, since the model aims at the prediction of thermodynamic properties of high-order systems using solely the information of binary systems. The interaction term $\Omega^{ij(O)}$ can be evaluated using the experimental data for activities in the $Ci_{ci}O_{ai}$-$Cj_{cj}O_{aj}$ binary system. In other words, the binary interaction parameters in equation (7) can be optimised using available experimental information. The choice of the Ω parameters in the use of equation (7) would depend on the system studied. In general, the first two to three parameters are sufficient to provide good model calculations for a binary system.

2.3. Standard State for SiO_2

It is well known that the basic building units of liquid silica are SiO_4^{4-} tetrahedra, which share corners with one another. On the other hand, the standard Gibbs energy of SiO_2, $G^O_{SiO_2}$ in equation (3) refers to a hypothetical state where silica is completely dissociated into Si^{4+} and O^{2-} ions. The Gibbs energy change for the standard state change from pure SiO_2 (network) to ionic SiO_2 (consisting of Si^{4+} and O^{2-}) has been evaluated by Lumsden /3/. Based on the silica saturated liquidus in the 'FeO'-SiO_2 system, he deduced the Gibbs energy change for the fusion of silica:

$$\mathrm{Si}\,O_2(solid) = \mathrm{Si}\,O_2(\text{ liquid consisting of } Si^{4+} \text{ and } O^{2-}) \qquad (8)$$

$$\Delta G_8 = 35600 - 7.53T \qquad \text{(J/mole)} \qquad (9)$$

A calculation based on the activities of 'FeO'-in the 'FeO'-SiO_2 system was made in the present work to estimate the Gibbs energy change for reaction (8). A value of 22000 J/mole was obtained for ΔG_8 in the temperature range of 1533-1673K. Comparison of this value with the value according to equation (9) in the same temperature range shows very good agreement. The choice of the 'FeO'-SiO_2 binary for the evaluation is due to the consideration that this system has been studied most extensively and the agreement between the experimental data reported by different research groups is very good. Moreover, the liquid phase has a very wide composition range, which is necessary for reliable calculation. However, no attempt was made to evaluate ΔG_8 as a function of temperature, since the activity of 'FeO'-does not show very strong temperature dependency in the 'FeO'-SiO_2 system. Instead, equation (9) was adopted.

3. MODEL APPLICATION

3.1. Binary Systems

Model calculations were carried out for three binary systems, viz. 'FeO'-SiO_2, MgO-SiO_2 and MnO-SiO_2.

3.1.1. 'FeO'-SiO$_2$ system

The 'FeO'-SiO$_2$ binary system in equilibrium with iron has been studied by a number of research groups /12-18/. In these studies, gas-slag equilibration techniques using CO-CO$_2$ /12/ or H$_2$-H$_2$O /13,14/ gas mixtures, EMF method /15,16/ and slag-metal equilibration techniques /17,18/ were employed to determine the 'FeO'-activities in the system. The studies of Schumann and Ensio /12/, Bodsworth /13/, Ban-Ya *et al.* /14/, Wijngaarden and Dippenaar /15/ and Wanibe *et al.* /16/ were all carried out below 1680 K, while Fujita and Maruhashi /17/ and Distin *et al.* /18/ studied this system at higher temperatures. The former carried out their measurements at 1833 K, the latter was able to determine the activities of 'FeO'-in this temperature range of 2058-2233 K by using levitation technique. A direct comparison of the experimental data by Fujita and Marushashi /17/ and Distin *et al.* /18/ with the experimental results at lower temperatures /12-16/ was found to be difficult. On the other hand, the experimental data obtained using different techniques show very good agreement except the results reported by Wanibe *et al.* /16/. Hence, the experimental results of Schumann and Ensio /12/, Bodsworth /13/, Ban-Ya *et al.* /14/ and Wijngaarden and Dippenaar /15/ were adopted in the model calculation. The model parameters optimised based on the 'FeO' activities are listed in Table 1. It should be mentioned that the model parameters listed in this table were all obtained using equation (5) referring pure liquid oxides as the standard states. In the case of SiO$_2$, the standard state was the hypothetical state where silica is completely dissociated into Si^{4+} and O^{2-} ions.

Figure 1 presents the comparison between evaluated 'FeO' activities with the experimental data /12-18/. The experimental data by Schumann and Ensio /12/, Bodsworth /13/, Ban-Ya *et al.* /14/ and Wijngaarden and Dippenaar /.15/, which were earlier employed for the

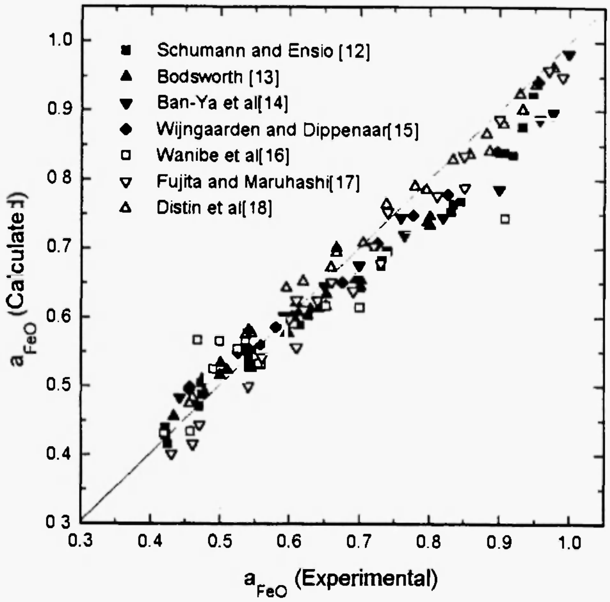

Fig. 1: Comparison between calculated activities of 'FeO' with the experimental data in the 'FeO'-SiO$_2$ system.

Table 1

Optimised model parameters

$\Omega_1^{Fe\,Si(O)} =$	-28128.2
$\Omega_3^{Fe\,Si(O)} =$	-4627.94
$\Omega_5^{Fe\,Si(O)} =$	20677.8
$\Omega_1^{Mg\,Si(O)} =$	-124943
$\Omega_3^{Mg\,Si(O)} =$	-64403.8
$\Omega_5^{Mg\,Si(O)} =$	-81919.9
$\Omega_1^{Mn\,Si(O)} =$	-104693
$\Omega_2^{Mn\,Si(O)} =$	17.2827
$\Omega_3^{Mn\,Si(O)} =$	-25956.7
$\Omega_5^{Mn\,Si(O)} =$	27334.6

All the model parameters are obtained using equation (5) referring pure liquid oxides as the standard states. In the case of SiO$_2$, the standard state is the hypothetical state where silica is completely dissociated into Si^{4+} and O^{2-} ions.

optimisation of the model parameters, are well reproduced by the model calculations. It is satisfactory to see that even the data at higher temperatures /17,18/, that were not included in the optimisation, are very well predicted by the model. Figure 1 also shows that the experimental results obtained by Wanibe *et al.* /16/ do not follow the trend of the other research groups.

The calculated activities of 'FeO'-and SiO_2 (referring to pure liquid FeO and pure solid SiO_2 respectively at the same temperature) are plotted in Figure 2 as functions of composition at different temperatures. These activity curves show that both a_{FeO} and a_{SiO_2} only slightly depend on temperature. In general, the activities tend towards ideality and decrease with the increasing temperature for a given slag composition. In view of the large number of experimental points, these data are not presented in Figure 2 for the sake of clarity.

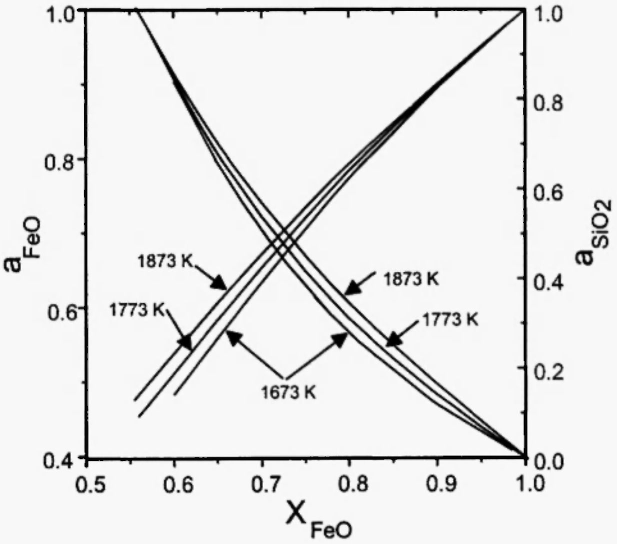

Fig. 2: Activities of 'FeO' and SiO_2 as functions of composition in the 'FeO'-SiO_2 system. The standard states are pure liquid 'FeO' and pure solid SiO_2.

3.1.2. MgO-SiO₂ system

The activities of SiO_2, a_{SiO_2} in this binary at 1873 K were measured by Rein and Chipman /19/ using slag-metal equilibration technique. They calculated a_{SiO_2} from the distribution of silicon between the slags and Fe-Si-C alloys saturated with either graphite or silicon. On the other hand, Kambayashi and Kato /20/ measured both a_{MgO} and a_{SiO_2} at the same temperature using high-temperature mass spectrometry. In view of the extremely low vapour pressures of MgO and SiO_2, these authors determined the activities of the two oxides from the measurements of the relative intensities of SiO and Mg based on the relation:

$$SiO_2(\text{solution})+Mg(\text{gas}) = MgO(\text{solution})+SiO(\text{gas})$$

The results of both research groups /19,20/ were employed in the present work. Three model parameters were optimised. These parameters are presented in Table 1. The Gibbs energy of fusion for MgO is presented in Table 2.

The calculated activities of the two oxides are plotted as functions of composition in Figure 3, where solid MgO and SiO_2 at the same temperature of the solution were taken as the standard states for magnesium oxide and silicon oxide, respectively. The experimental results /19,20/ are also included in the same figure for comparison. It is seen that in the case of both a_{MgO} and a_{SiO_2}, the results of model calculations agree well with the experimental data.

3.1.3. MnO-SiO₂ system

Four experimental studies of the MnO activities in the MnO-SiO_2 system are available in the literature /21-24/. Schenck *et al.* /21/ determined the MnO activities by equilibrating the liquid slag with Fe-Mn liquid solution in a graphite crucible. On the other hand,

Table 2
Gibbs energy of fusion

Reaction	Gibbs energy of fusion	Reference
MgO(s)=MgO(l)	$\Delta G^0_{MgO} = 77822 - 25.063 \cdot T$	34
MnO(s)=MnO(l)	$\Delta G^0_{MnO} = 43932 - 20.772 \cdot T$	34

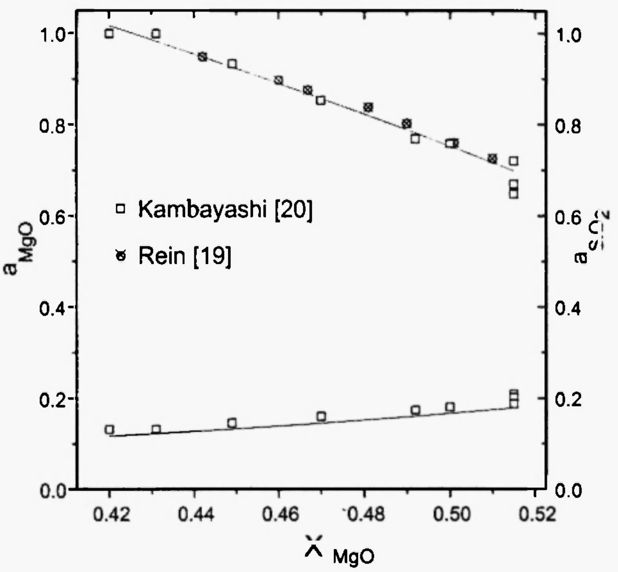

Fig. 3: Activities of MgO and SiO_2 as functions of composition in the MgO-SiO_2 system at 1873 K. The standard states are pure solid for both MgO and SiO_2.

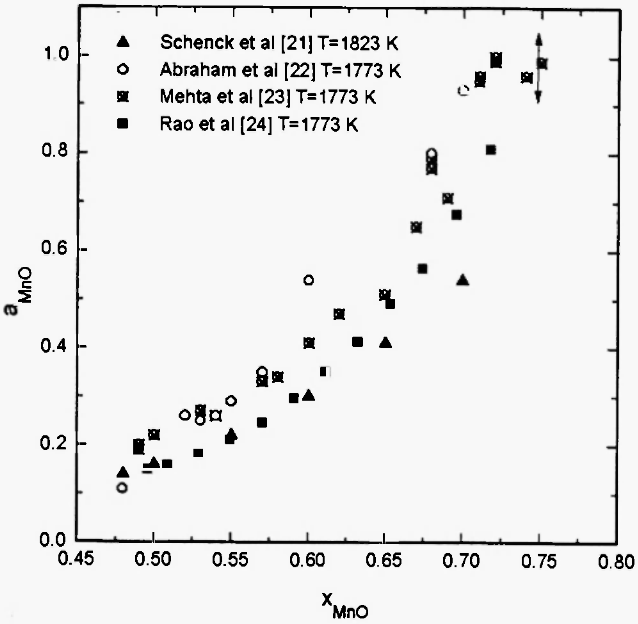

Fig. 4: Activities of MnO in the MnO-SiO_2 system at 1773 K and 1833 K. The arrow represents the MnO saturation at 1773 K. The standard state is pure solid MnO.

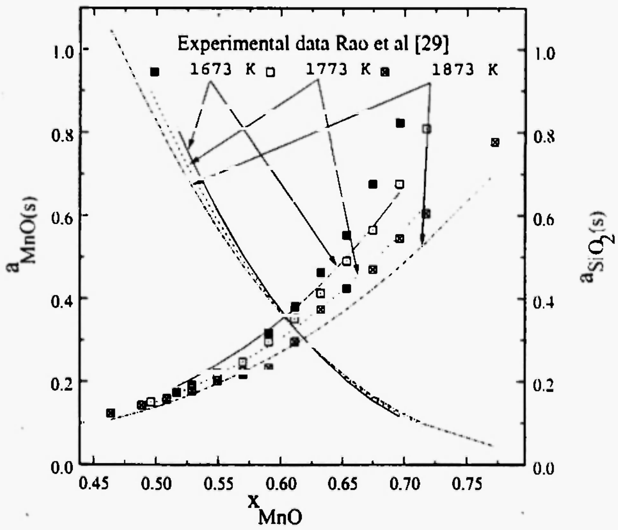

Fig. 5: Activities of MnO and SiO_2 as functions of composition in the MnO-SiO_2 system. The standard states for MnO and SiO_2 are pure solid MnO and SiO_2 respectively.

the other research groups /22-24/ equilibrated the liquid slag with a gas mixture of fixed oxygen partial pressure and a Pt-Mn foil immersed in the melt to determine MnO activities. While Abraham *et al.* /22/ and Mehta and Richardson /23/ used a H_2+CO_2+N_2 gas mixture, Rao and Gaskell /24/ employed CO-CO_2. The experimental data reported by different authors /21-24/ are compared in Figure 4, where solid manganese oxide at the same temperature is taken as the standard state. The boundaries of the MnO saturation /25/ at 1773 K is also presented in the same figure. It is seen that while the experimental results by Schenck *et al.* /21/, Mehta and Richardson /23/ and Rao and Gaskell /24/ are in reasonable agreement, the data reported by Abraham *et al.* /22/ appear to be on the high activity side. This is especially true in the composition range of $0.6 < X_{MnO} < 0.7$. In view of the agreement of the experimental data obtained by the former three research groups using different experimental approaches /21,23,24/, their data were employed for the model calculations. The optimised model parameters are also included in Table 1. The calculated activities of MnO and SiO_2 are plotted as functions of composition in Figure 5. The standard states for MnO and SiO_2 are solid manganese oxide and silica at the same temperature. The Gibbs energy of fusion for MnO is presented in Table 2. The experimental results by Rao and Gaskell are presented in the same figure for comparison. For the sake of clarity the experimental data by Schenck *et al.* /21/ and Mehta and Richardson /23/ are not included in this figure. It is seen that the model calculations are in agreement with the experimental data.

3.2. Ternary Systems

3.2.1. MgO-'FeO'-SiO_2 system

The MgO-'FeO'-SiO_2 system in equilibrium with iron can be expressed as:

$$(Mg^{2+}, Fe^{2+}, Si^{4+})_pO_q^{2-}$$

In this system, p is always equal to one. On the other hand, q varies with composition. Three binary interactions could be encountered in this system, viz. Mg^{2+}-Si^{4+}, Fe^{2+}-Si^{4+} and Mg^{2+}-Fe^{2+}. While the first two have been obtained in the MgO-SiO_2 and 'FeO'-SiO_2 systems respectively, the interaction between Mg^{2+} and Fe^{2+} is not available due to the lack of the experimental data for the MgO-'FeO' system. The MgO-'FeO' binary shows only a slight positive deviation from ideality in the solid solution /26,27/. It would be a reasonable approximation to assume that the MgO-'FeO' liquid solution is ideal. Hence, no interaction between Mg^{2+} and Fe^{2+} was considered in the model calculation.

The activities of 'FeO', MgO and SiO_2 in the MgO-'FeO'-SiO_2 system were calculated using the model parameters for the Mg^{2+}-Si^{4+} and Fe^{2+}-Si^{4+} interactions listed in Table 1. The calculated iso activity curves for a_{FeO}, a_{MgO} and a_{SiO_2} are plotted in Figures 6a-6c respectively. The standard states for 'FeO', MgO and SiO_2 are the pure oxides in their stable states at the same temperature of the solution. Ban-Ya and Shim /4/ have measured the activities of 'FeO' in the MgO-'FeO'-SiO_2 slags at 1873 K using gas-slag equilibration techniques. Their results are also included in Figure 6a for comparison. It is seen that the predicted iso activity lines are in good agreement with the experimental data, being well within the experimental uncertainties. It should be mentioned that some of the experimental data of Ban-Ya and Shim /4/ fall in the two-phase region according to the phase diagram /28/. No attempt was made to evaluate the activities beyond the homogeneous liquid phase region in the present study. Based on the measurements of the activities of 'FeO' along the MgO and SiO_2 saturation lines, Kojima *et al.* /29/ constructed iso activity curves for 'FeO' in this ternary system. Their

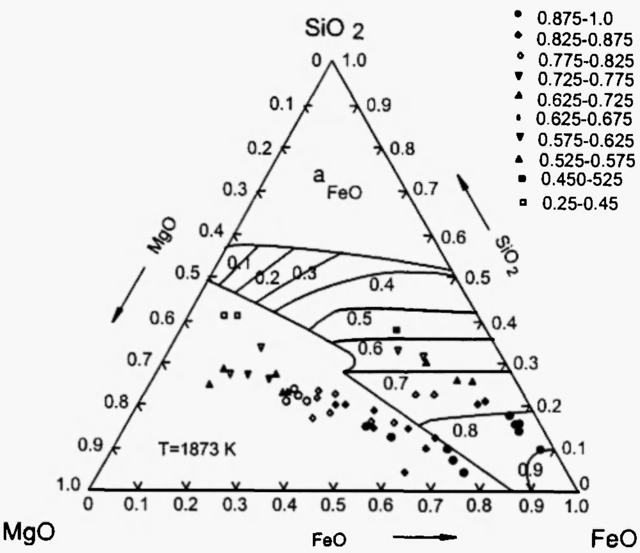

Fig. 6a: Calculated and experimentally /4/ determined activities of 'FeO' in the MgO-'FeO'-SiO_2 system at 1873 K. The standard state is pure liquid 'FeO'.

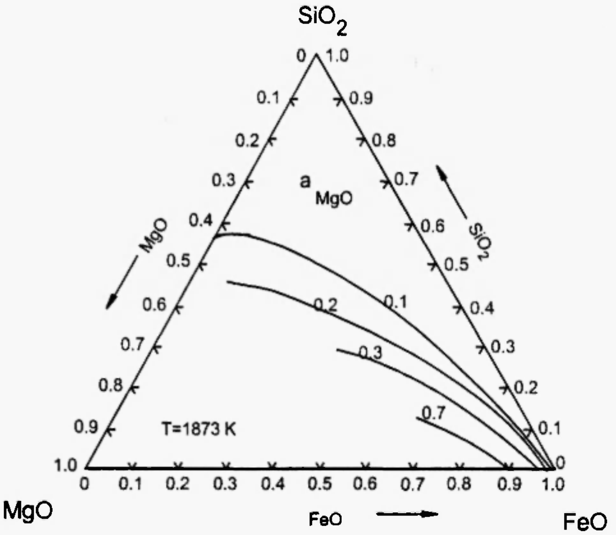

Fig. 6b: Calculated activities of MgO in the Mgo-'FeO'-SiO_2 system at 1873 K. The standard state is pure solid MgO.

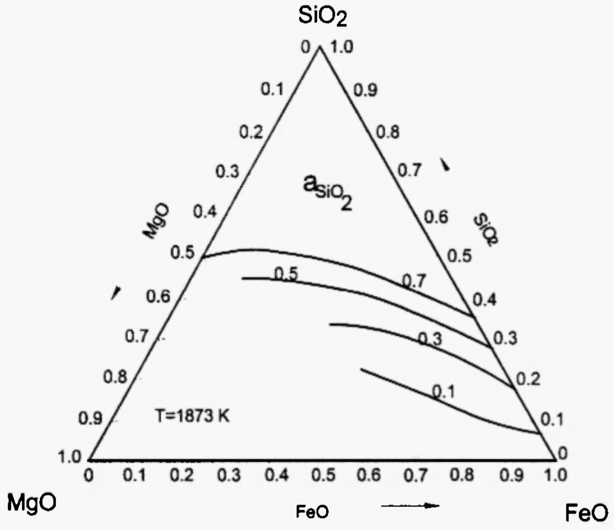

Fig. 6c: Calculated activities of SiO_2 in the MgO-'FeO'-SiO_2 system at 1873 K. The standard state is pure solid SiO_2.

results are reproduced in Figure 7. Comparison of Figure 6a and Figure 7 shows that the results of the present authors and Kojima *et al.* /29/ have the same trend, whilst the activity values calculated in the present work are somewhat higher in the low activity region. It is noted that the MgO saturation boundary adopted in Figure 7 is more close to the pure MgO compared to the line recommended by the phase diagram /28/. The use of different phase diagrams could be one of the reasons for the disagreement in the low activity area. More work is needed in order to clarify this situation.

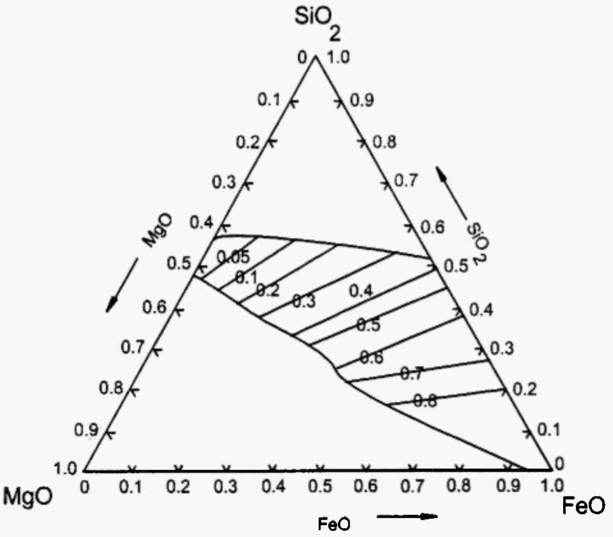

Fig. 7: Iso activities of 'FeO' in the MgO-'FeO'-SiO_2 system at 1873 K suggested by Kojima *et al.* /29/. The standard state is pure liquid 'FeO'.

3.2.2. MnO-'FeO'-SiO_2 system

The MnO-'FeO'-SiO_2 system is in equilibrium with iron. Similar to the case of the MgO-'FeO'-SiO_2 system, the stoichiometric number p in the expression:

$$(Mn^{2+}, Fe^{2+}, Si^{4+})_pO_q^{2-}$$

is always one, whilst q varies with composition in the MgO-'FeO'-SiO_2 ternary. The interactions of Mn^{2+}-Si^{4+}, Fe^{2+}-Si^{4+} in the presence of O^{2-} have been obtained in the MnO-SiO_2 and 'FeO'-SiO_2 binaries, respectively. Fujita and Maruhashi /30/ have found that the liquid 'FeO'-MnO binary system behaves ideally. Hence, the interaction between Mn^{2+} and Fe^{2+} is not considered in the model calculation for the MnO-'FeO'-SiO_2 system.

The calculated activities of MnO, 'FeO' and SiO_2 at 1833 K are presented in Figures 8a-8c, respectively. Pure MnO, 'FeO' and SiO_2 at their stable state and the same temperature are chosen as the standard states for the corresponding components. The activities of the component oxides in this ternary have been studied by several research groups /30-33/. The experimental data for a_{FeO} and a_{MnO} by Fujita and Maruhashi /30/ are incorporated in Figures 8a and 8b for comparison. These authors determined a_{FeO} and a_{MnO} in the MnO-'FeO'-SiO_2 ternary slags at 1833 K using slag-metal equilibration method. It is seen in Figures 8a and 8b that the model predictions are in agreement with the experimental data in the case of both a_{FeO} and a_{MnO}. In general, the present iso activity curves are in agreement with those suggested by Sommerville *et al.* /31/ as well as by Ban-Ya and Yuge /32/. As an example, the iso activity lines of MnO at 1823 K reported by Sommerville *et al.* /31/ are reproduced in Figure 9. These iso activity lines are in accordance with the present results shown in Figure 8b. The activities of 'FeO' along the MnO saturated boundary in the MnO-'FeO'-SiO_2 ternary system have been determined by Fischer and Bardenheuer /33/. Their experimental data are compared with the present model predictions at 1873 K in Figure 10. The good

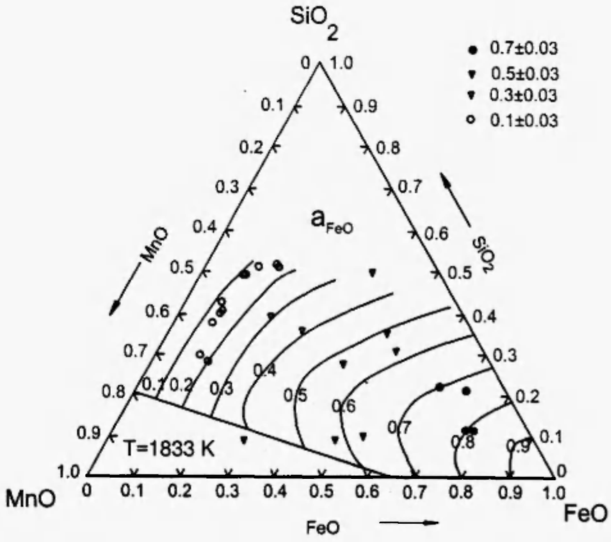

Fig. 8a: Calculated and experimentally determined /30/ activities of 'FeO' in the MnO-'FeO'-SiO_2 system at 1833 K. The standard state is pure liquid 'FeO'.

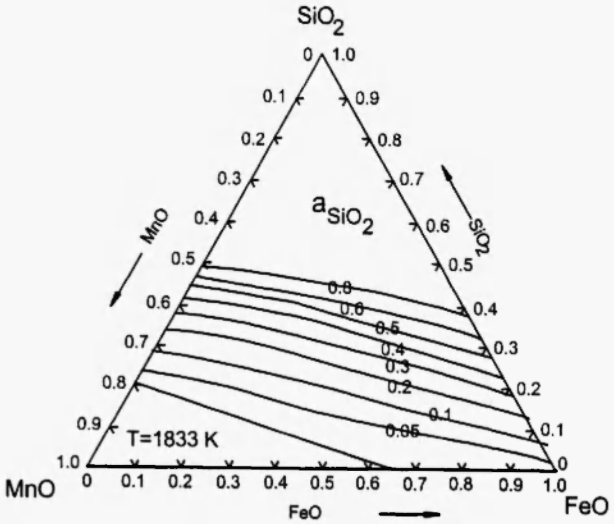

Fig. 8c: Calculated activities of SiO_2 in the MnO-'FeO'-SiO_2 system at 1833 K. The standard state is pure solid SiO_2.

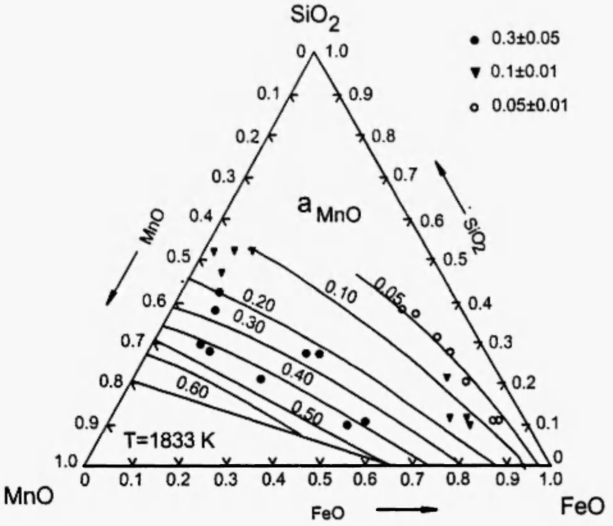

Fig. 8b: Calculated and experimentally determined /30/ activities of MnO in the MnO-'FeO'-SiO_2 system at 1833 K. The standard state is pure solid MnO.

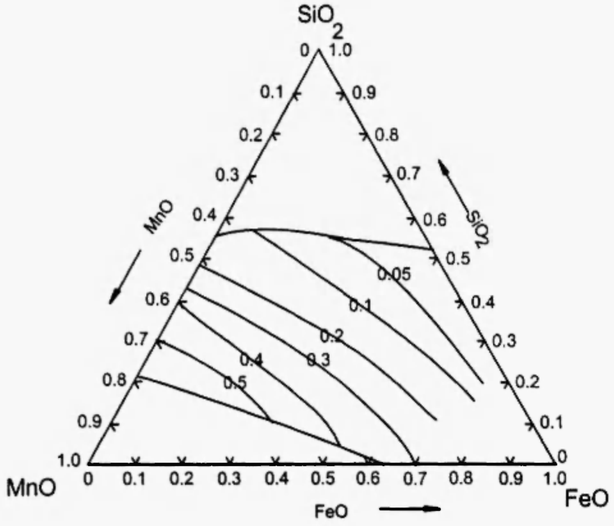

Fig. 9: Iso activity lines of MnO in the MnO-'FeO'-SiO_2 system at 1823 K suggested by Sommerville *et al.* /31/. The standard state is pure solid MnO.

agreement again shows the reliability of the present model approach.

4. DISCUSSION

The difference between the use of equation (1) and the formulation of silicate melts using complex anionic

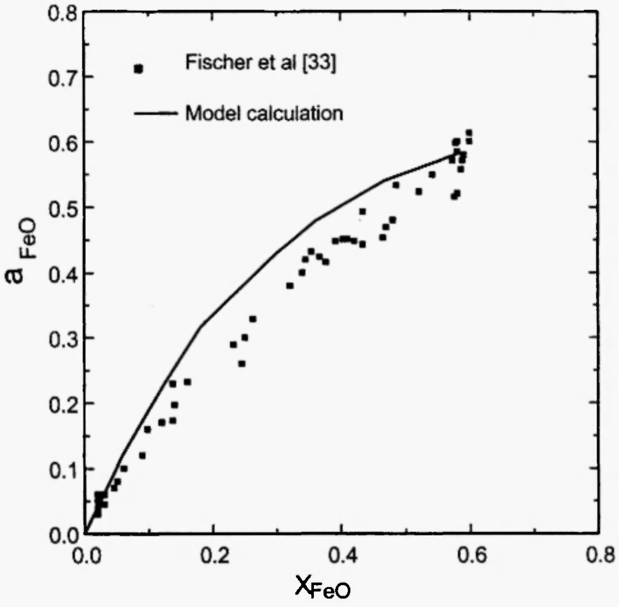

Fig. 10: Activities of 'FeO' along the MnO saturated boundary in the 'FeO'-MnO-SiO_2 ternary system at 1873 K. The standard state is pure liquid 'FeO'.

species, like SiO_4^{4-}, is only the way of looking at the nature of the ionic solutions. The model based on equation (1) pictures an ionic solution as an oxygen anion matrix with different cations including Si^{4+} distributed in it. The occurrence and the fractions of the complex ions SiO_4^{4-}, $Si_2O_7^{6-}$, $Si_3O_{10}^{8-}$, cyclic polymers and even a three-dimensional network of bridged silica tetrahedra will of course determine the oxygen matrix and the distribution of the cations. However, the experimental information is far from sufficient to support model calculations for the fractions of the polymers in multi-component melts. The present approach avoids the difficulties in attributing the effect of mixing to two unknown factors, namely the fractions of the polymers and the interactions between them. Instead, only the interactions between different cations in the presence of O^{2-} are considered. The fractions of the cations can easily be calculated from the mole fractions of the component oxides. Since the next nearest neighbour interactions are considered as a function of composition, the structural factors of the ionic liquid are included in the interactions mathematically.

The comparison of the model predictions with the experimental data in the case of both the MgO-'FeO'-SiO_2 and the MnO-'FeO'-SiO_2 systems shows that the activities of the oxide components in a ternary system can be successfully predicted using solely the information of the binary systems on the basis of the present model. The model would be a valuable tool for evaluation of activities of the oxide components in high order systems. The success of the model calculations implies that equation (1) could provide a reasonable description for ionic solutions. It also proves the validity of Richardson's conclusion regarding the dominant role of the next nearest neighbour interactions in the solution thermodynamics.

It is noted that the two ternary systems studied involve only the cations Fe^{2+}, Mg^{2+}, Mn^{2+} and Si^{4+}. Among these cations, Fe^{2+}, Mg^{2+} and Mn^{2+} share similarities. It would be interesting to see if the present approach can also be applied to the ternary and higher order systems involving other cations like Ca^{2+} and Al^{3+}. In the case of Ca^{2+}, Richardson /9/ has encountered difficulties in his calculation for systems involving CaO, since Ca^{2+} has a quite different radius, much bigger than Fe^{2+}, Mg^{2+} and Mn^{2+}. In the case of Al^{3+}, Al_2O_3 is an amphoteric oxide, which might complicate the distribution of the cations in the oxygen matrix and the interactions between different cations. An examination of the model calculation involving these oxides would reveal the applicability of the model to such systems. Model calculations for the systems involving CaO and Al_2O_3 are currently being carried out in the present laboratory.

It should be mentioned that the Gibbs energy change for fusion of silica, namely equation (9), was derived by Lumsden /3/ based on the silica saturated liquidus in the FeO-SiO_2 system. Since the activities do not show very strong temperature dependence, the temperature dependence in the expression for ΔG_8 might involve some uncertainty. The value of ΔG_8 would have an important impact on the activity calculations. It is felt that equation (9) need to be verified in future on the basis of more binary silicate systems.

SUMMARY

In this work, a thermodynamic model has been applied to two ternary silicate systems, 'FeO'-MgO-SiO_2 and 'FeO'-MnO-SiO_2. The model pictures oxide melts including silicate solutions as an O^{2-} matrix with different cations distributed in it. It avoids the difficulties in choosing the complex ionic species and the evaluation of their fractions. Only the next nearest neighbour interactions, viz. the interactions between different cations in the presence of oxygen, are considered to be important in the solution thermodynamics. Assessments have been made for the 'FeO'-SiO_2, MgO-SiO_2 and MgO-SiO_2 binary systems based on the literature data. The optimised binary interaction parameters have been employed for the calculation of the oxide activities in the ternary systems 'FeO'-MgO-SiO_2 and 'FeO'-MnO-SiO_2. The predicted activities have been found to be in good agreement with the literature data.

REFERENCES

1. G.W. Toop and C.S. Samis. *Trans. TMS-AIME*, **224**, 878-887 (1962).
2. C.R. Masson, *J. Iron Steel Inst.*, **210**, 89-96 (1972).
3. J. Lumsden. *Int. Symp., Physical Chemistry of Process Metallurgy*, Part 1, AIME, 1959; 165-205.
4. S. Ban-Ya and J.-D. Shim. *Canadian Metall. Quarterly*, **21**, 319-328 (1982).
5. M. Blander and A.D. Pelton. *Geochemica et Cosmochimica Acta*, **51**, 85-95 (1987).
6. M. Hillert, B. Jansson, B. Sundman and J. Ågren. *Metall. Trans.*, **16A**, 261-266 (1985).
7. H. Gaye and J. Welfringer. *Second Int. Symp., Metallurgical Slag and Fluxes*, Nevada, 1984; 357-375.
8. M. Selleby, *Metall. Trans.*, **28B**, 577-596 (1997).
9. F.D. Richardson. *Trans. Faraday Soc.*, **52**, 1312-1224 (1956).
10. J. Bygdén, Du Sichen and S. Seetharaman. *Steel Research*, **10**, 421-428 (1994).
11. M. Temkin. *Acta Phys. Chim. U.R.S.S.*, **20**(4), 411-420 (1945).
12. R. Schumann and P.J. Ensio, *Trans. AIME*, **191**, 401-411 (1951).
13. C. Bodsworth, *J. Iron Steel Inst.*, **193**, 13-24 (1959).
14. S. Ban-Ya, A. Chiba and A. Hikosaka. *Tetsu-to-Hagane*, 66 (10), 1484-1493 (1980).
15. M. van Wijngaarden and R. Dippenaar. *J. S. Afr. Inst. Min. Metall.*, **86** (11), 443-453 (1986).
16. Y. Wanibe, Y. Yamauchi, K. Kawai and H. Sakao. *Arch. Eisenhuttenwes.*, 44 (9), 711-717 (1973).
17. H. Fujita, Y. Iritani and S. Maruhashi. *Tetsu-to-Hagane*, **54**, 359-370 (1968).
18. P.A. Distin, S.G. Whiteway and C.R. Masson. *Can. Met. Quart.*, **10**, 73-78 (1971).
19. H.R. Rein and J. Chipman, *Trans. Metall. SOC AIME*, **233**, 415-425 (1965).
20. S. Kambayashi and E. Kato. *J. Chem. Thermodynamics*, **15**, 701-707 (1983).
21. H. von Schenck, M.G. Frohberg and T. El Gammal. *Arch. Eisenhuttenwes.*, **32**, 509-511 (1961).
22. K.P. Abraham, M.W. Davies and F.D. Richardson. *J. Iron Steel Inst.*, 196, 82-89 (1960).
23. S.R. Mehta and F.D. Richardson. *J. Iron Steel Inst.*, **203**, 524-528 (1965).
24. B.K.D.P. Rao and D.R. Gaskell. *Metall. Trans.*, **12**b, 311-317 (1981).
25. F.P. Glasser. *Am. J. Sci.*, **256**(6), 398-412 (1958).
26. H.J. Engell. *Z. Phys. Chem. N.F.*, **35**, 192-195 (1962).
27. W.C. Hahn, Jr. and A. Muan. *Trans. Metall. SOC AIME*, **224**, 416-421 (1962).
28. *Slag Atlas*, 2nd ed., Verein Deutscher Eisenhüttenleute ed., Verlag Stahleisen GmbH, D-Düsseldorf, Germany, 1995; 142.
29. V.Y. Kojima, M. Inouye and K. Sano. *Arch. Eisenhüttenw.*, **40**, 37-40 (1969).
30. H. Fujita and S. Maruhashi. *Tetsu-To-Hagane*, **56**(7), 830-854 (1970).
31. D. Sommerville, I. Ivanchev and H.B. Bell. *Proc. Int. Symp. Metall. Chem. Application in Ferrous Metallurgy*, The Iron and Steel Inst., Sheffield, 1971; 23-25.
32. S. Ban-Ya, M. Hino and N. Yuge. *Iron and Steel Inst. Japan*, **71**, 853-860 (1985).
33. W.A. Fischer and P.W. Bardenheuer. *Arch. Eisenhüttenw.*, **39**, 637-643 (1968).
34. I. Barin, F. Sauert, E. Schultze-Rhonhof and W. Shu Sheng. *Thermochemical Data of Pure Substances*, Second Edition, VCH Verlagsgesellschaft mbH, Weinheim, Germany, 1993.